

Microscopic Mass Transfer of Uranium in Contaminated Sediments at Hanford Site

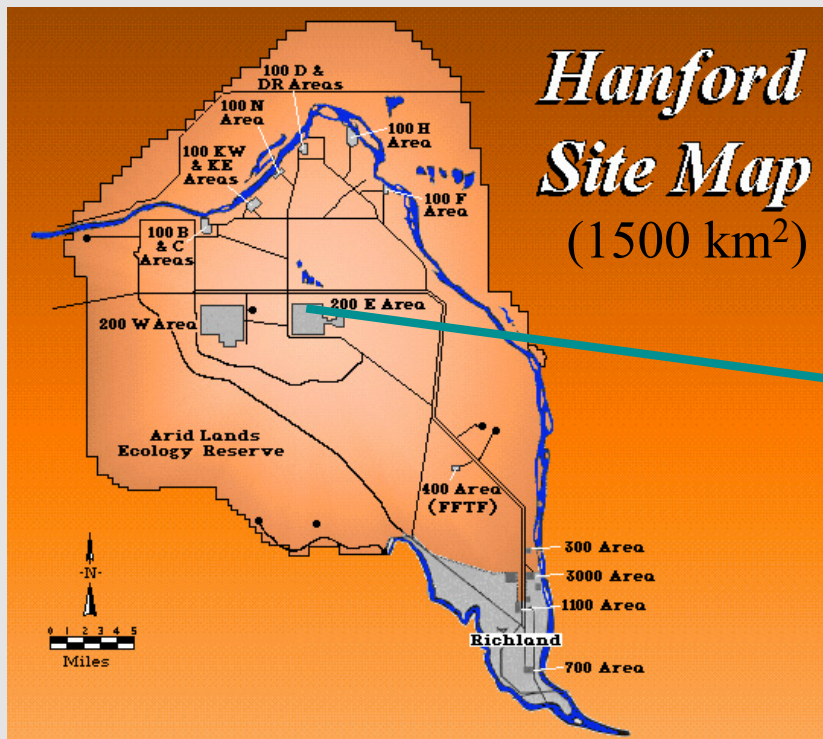
Chongxuan Liu, John Zachara, James McKinley, Paul Majors, and Sebastien Keristi

Pacific Northwest National Laboratory

DOE ERSP 2007 Annual PI Meeting, VA, April 18, 2007

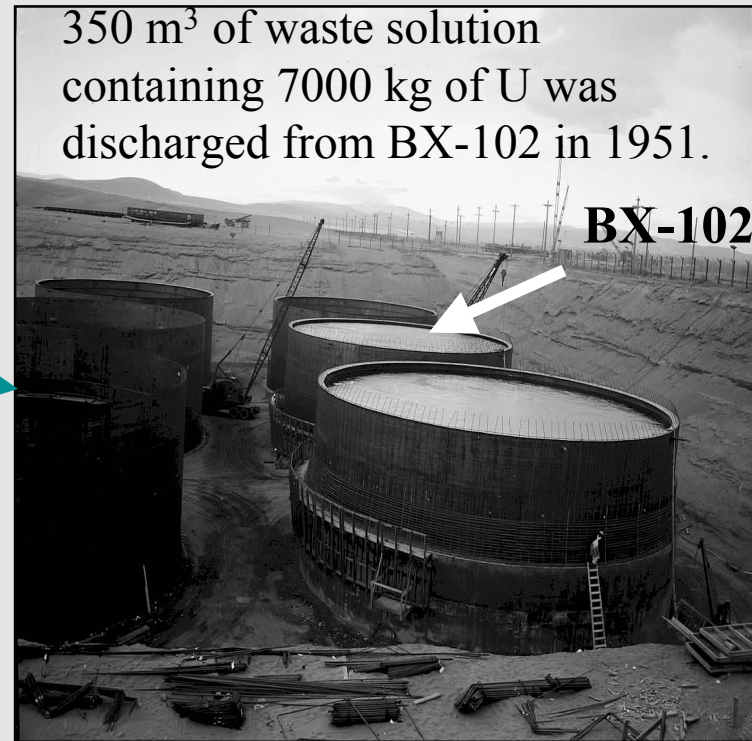
Hanford Site

Hanford Site



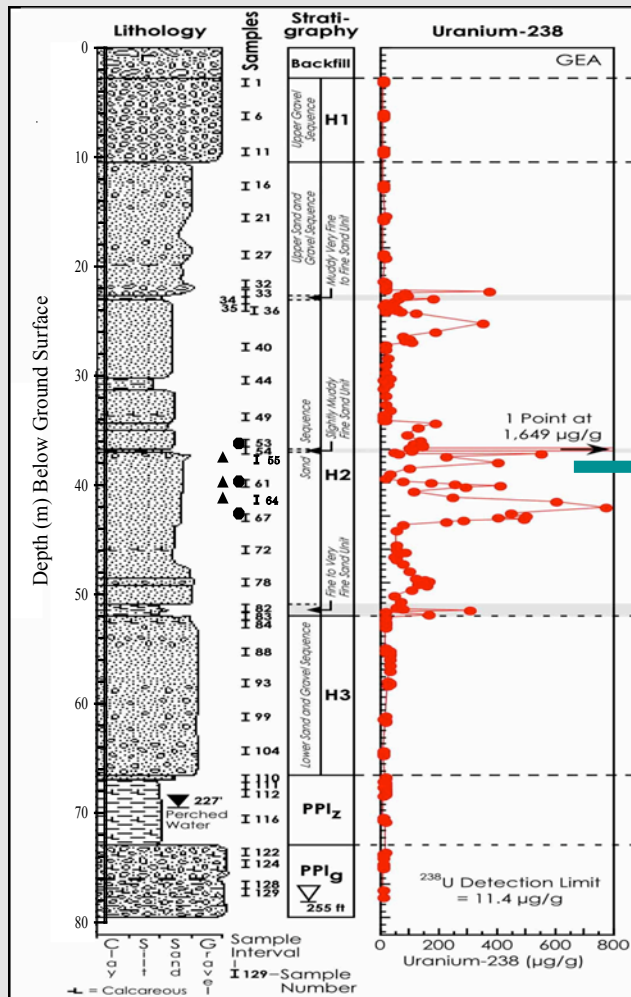
BX Tank Farm

350 m³ of waste solution containing 7000 kg of U was discharged from BX-102 in 1951.

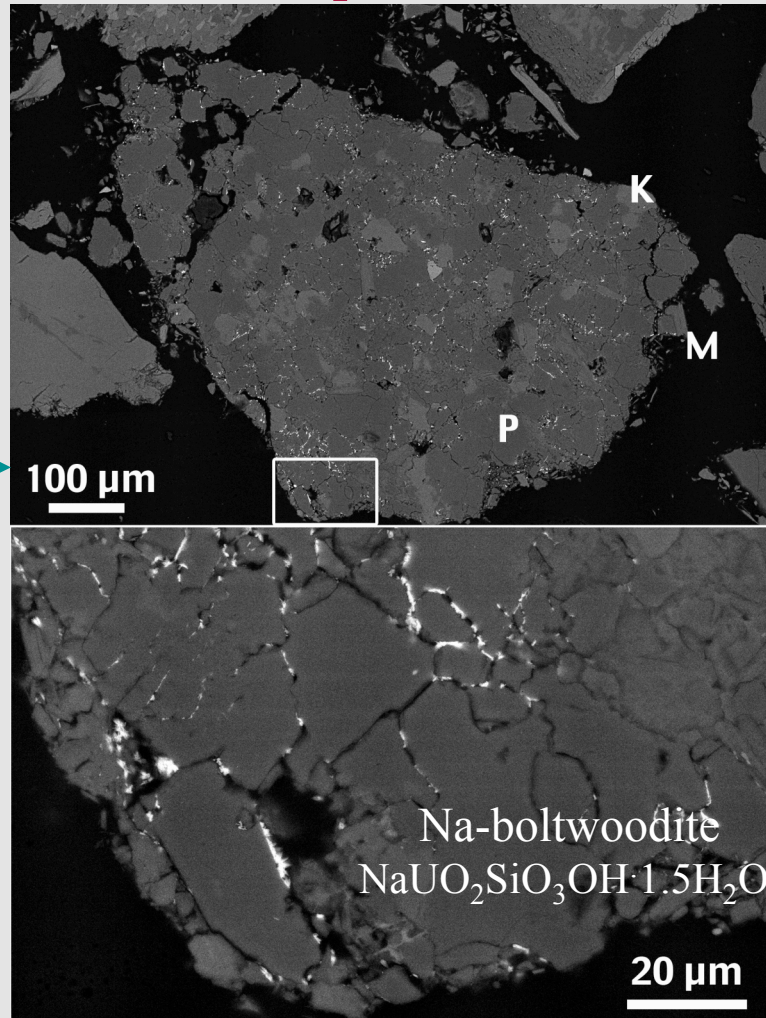


Uranium Distribution

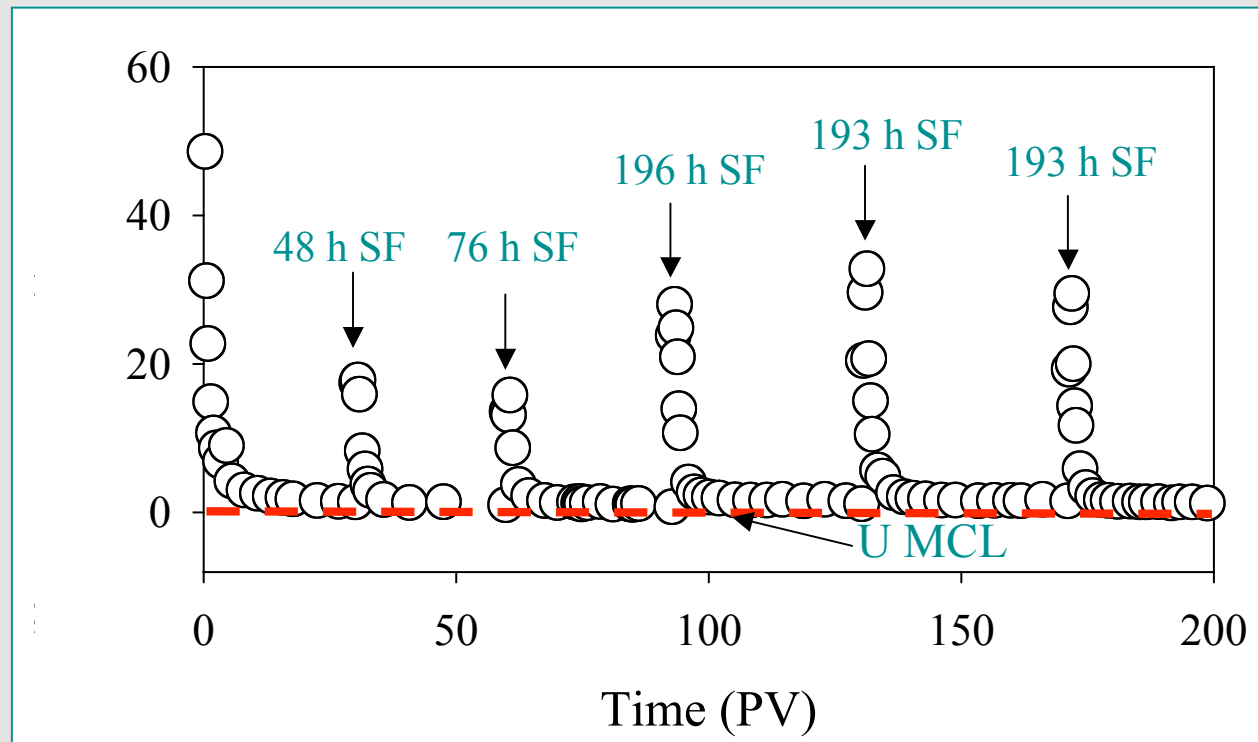
U Profile beneath BX-102



Intra-feldspar U distribution



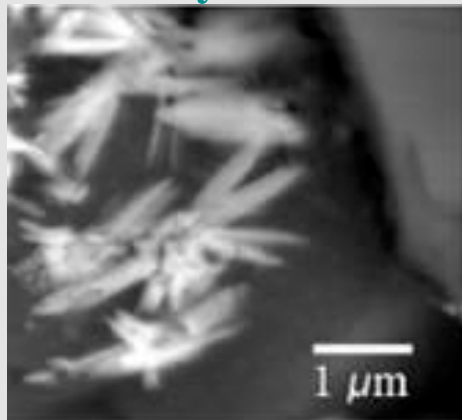
Kinetic Release of U(VI) from BX Sediments



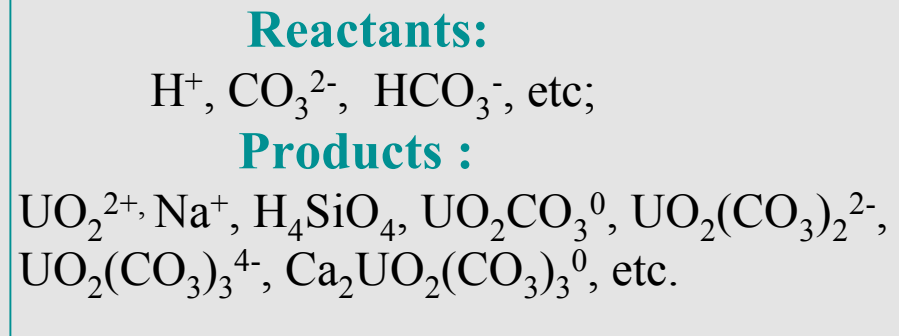
- Sediment U was leachable with Hanford SGW ($I = 0.05$ M, pH 8.0, equilibrium with calcite and air- CO_2 ,);
- Stop-flow (SF) events showed the kinetic behavior of U(VI) release;
- Effluent U(VI) was above U MCL.

Conceptual Microscopic Mass Transfer Model

Uranyl source



Dissolution

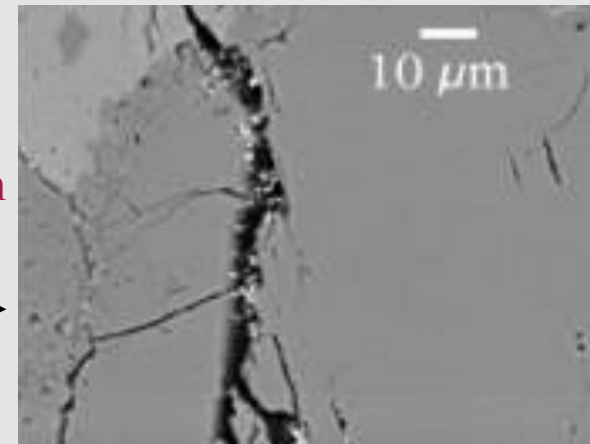


Diffusion to
microfracture network

Bulk/mobile domain:

- Advection, Dispersion,
Biogeochemical reactions:
- U(VI) complexation under MNA;
 - Microbial reduction;
 - U(VI) precipitation reactions.

Reactive diffusion
in microfractures



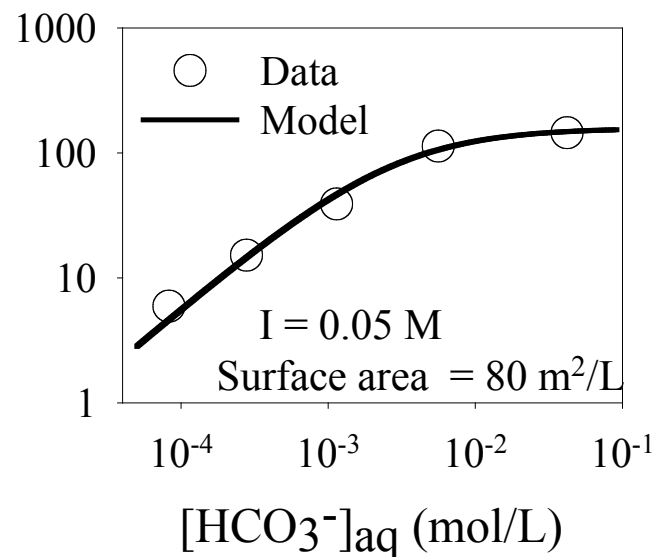
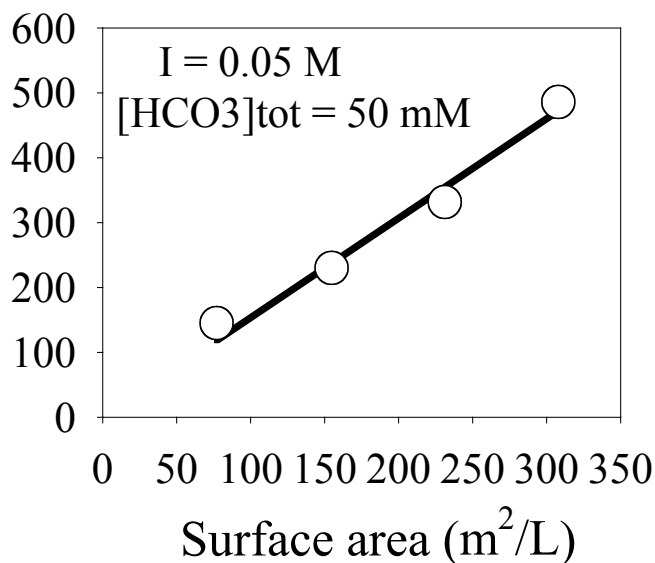
Outline

- Na-boltwoodite dissolution kinetics;
- Intragrain diffusion properties: NMR characterization and molecular simulation;
- Microscopic mass transfer model by coupling dissolution reaction and diffusion.

Research Questions

- Rate-limiting process: dissolution kinetics or diffusion?
- The importance of coupling dissolution reaction and diffusion?

Kinetics of Na-Boltwoodite Dissolution

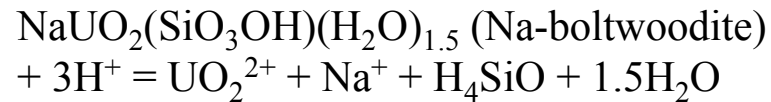


$$\text{Rate} = kA\rho_b \frac{[\text{HCO}_3^-]}{K_s + [\text{HCO}_3^-]} \left[1 - \left(\text{IAP} / K_{sp} \right)^n \right]$$

k : rate constant (5.69×10^{-10} mol/m²/s); A : specific surface area (30.8 m²/g); ρ_b : solid water ratio (g/L); K_s : half velocity constant (2.74 mmol/L); IAP: ion activity product; K_{sp} : solubility ($\log K_{sp} = 5.85$); and n : rate order ($n = 0.2$).

Kinetic Model of Na-Boltwoodite Dissolution

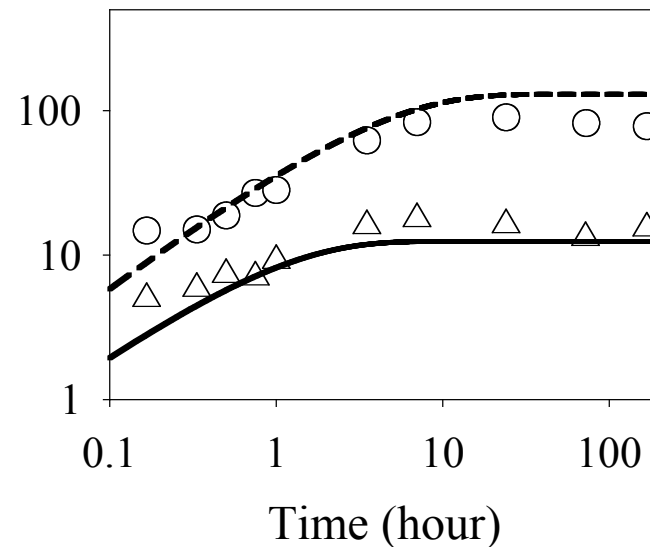
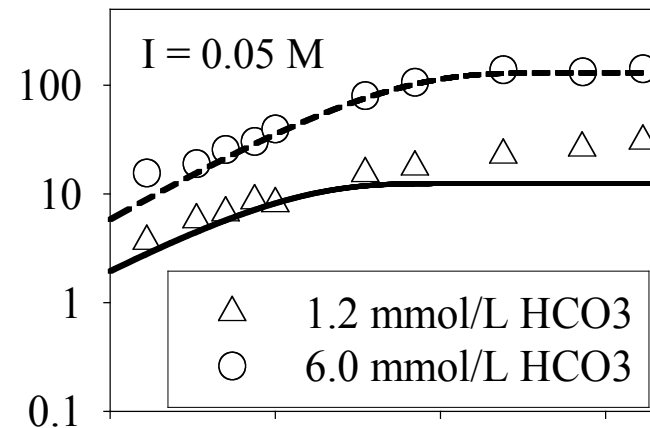
Kinetic reaction:



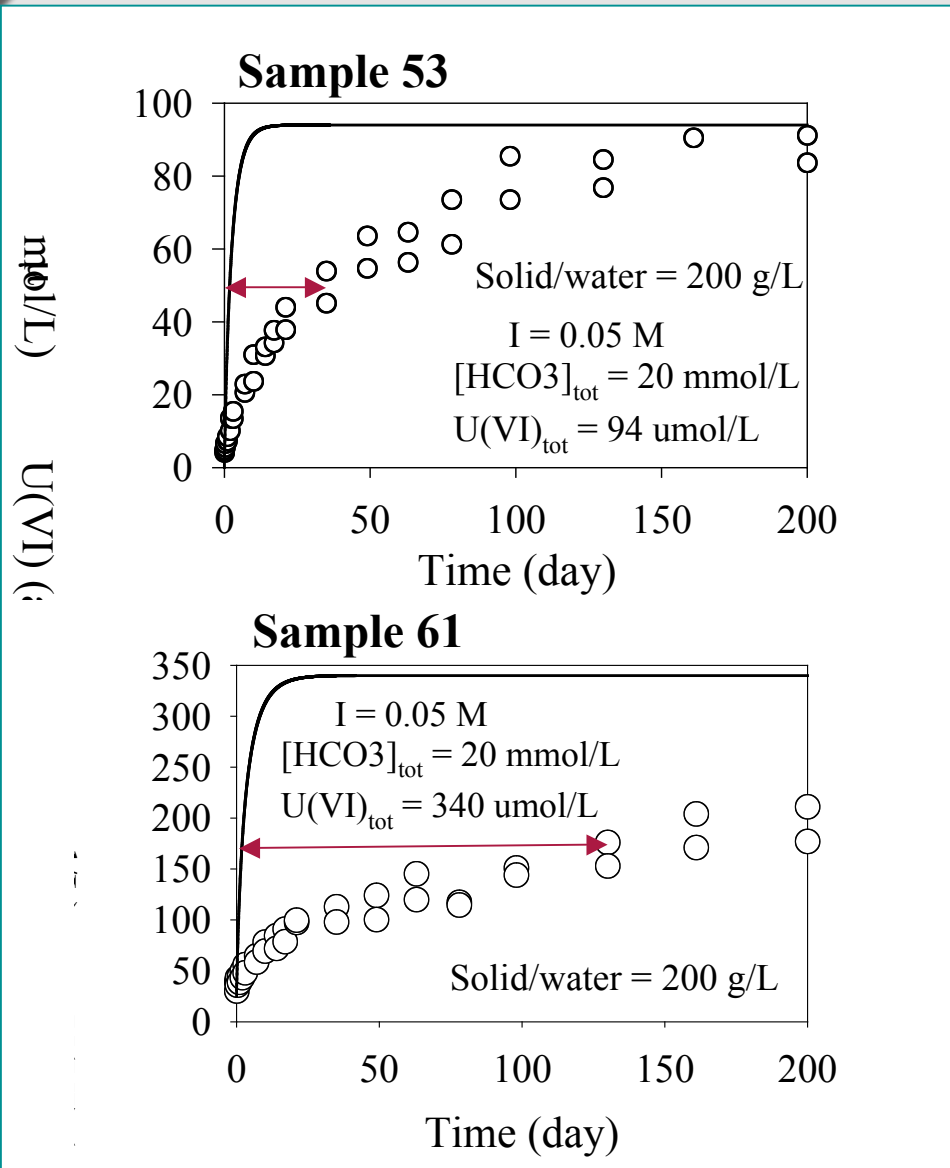
$$\text{Rate} = kA\rho_b \frac{[\text{HCO}_3^-]}{K_s + [\text{HCO}_3^-]} \left[1 - \left(\text{IAP} / K_{sp} \right)^{-1} \right]$$

Equilibrium reactions:

	log K (I=0)
$\text{UO}_2^{2+} + \text{H}_2\text{O} = \text{UO}_2\text{OH}^+ + \text{H}^+$	-5.25
$\text{UO}_2^{2+} + 2\text{H}_2\text{O} = \text{UO}_2(\text{OH})_2(\text{aq}) + 2\text{H}^+$	-12.15
$\text{UO}_2^{2+} + 3\text{H}_2\text{O} = \text{UO}_2(\text{OH})_3^- + 3\text{H}^+$	-20.25
$\text{UO}_2^{2+} + 4\text{H}_2\text{O} = \text{UO}_2(\text{OH})_4^{2-} + 4\text{H}^+$	-32.40
$2\text{UO}_2^{2+} + \text{H}_2\text{O} = (\text{UO}_2)_2\text{OH}^{3+} + \text{H}^+$	-2.70
$2\text{UO}_2^{2+} + 2\text{H}_2\text{O} = (\text{UO}_2)_2(\text{OH})_2^{2+} + 2\text{H}^+$	-5.62
$\text{UO}_2^{2+} + \text{CO}_3^{2-} = \text{UO}_2\text{CO}_3(\text{aq})$	9.94
$\text{UO}_2^{2+} + 2\text{CO}_3^{2-} = \text{UO}_2(\text{CO}_3)_2^{2-}$	16.61
$\text{UO}_2^{2+} + 3\text{CO}_3^{2-} = \text{UO}_2(\text{CO}_3)_3^{4-}$	21.84
$2\text{Ca}^{2+} + \text{UO}_2^{2+} + 3\text{CO}_3^{2-} = \text{Ca}_2\text{UO}_2(\text{CO}_3)_3$	29.80
$\text{UO}_2^{2+} + \text{NO}_3^- = \text{UO}_2\text{NO}_3^+$	0.30



U(VI) Dissolution from BX Sediments



➤ Dissolution model over-predicted experimental data about 2 orders of magnitude in time scale.

➤ Time scale (half life):
 Model Experimental

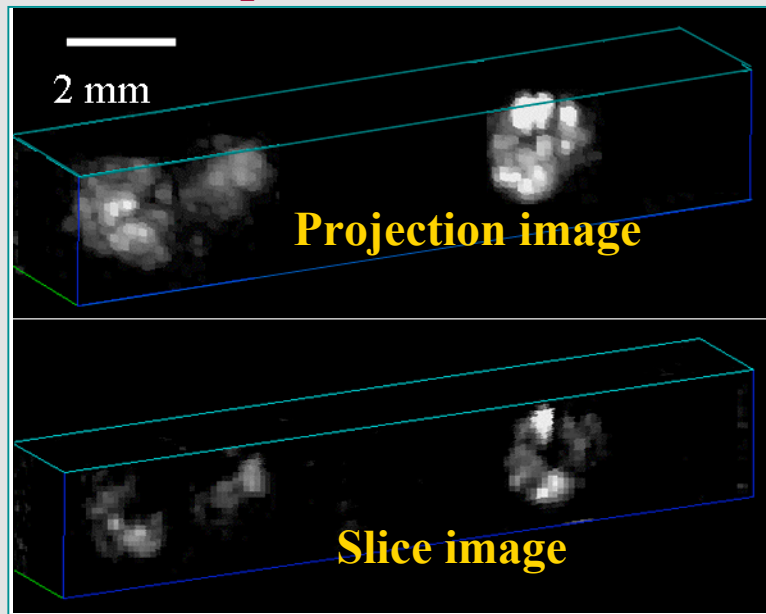
S53	40 hour	40 day
S61	44 hour	140 day

➤ Diffusion is rate-limiting?

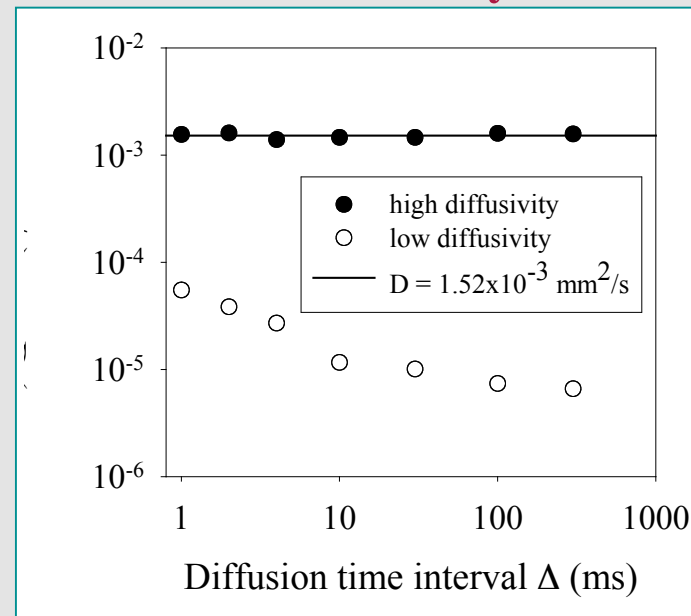
Characterization of Intragrain Diffusion

NMR-PGSE method was used to measure intragrain diffusion properties in Hanford feldspar grains (WRR, Liu et al, 2006)

MRI of H₂O distribution



Measured diffusivity



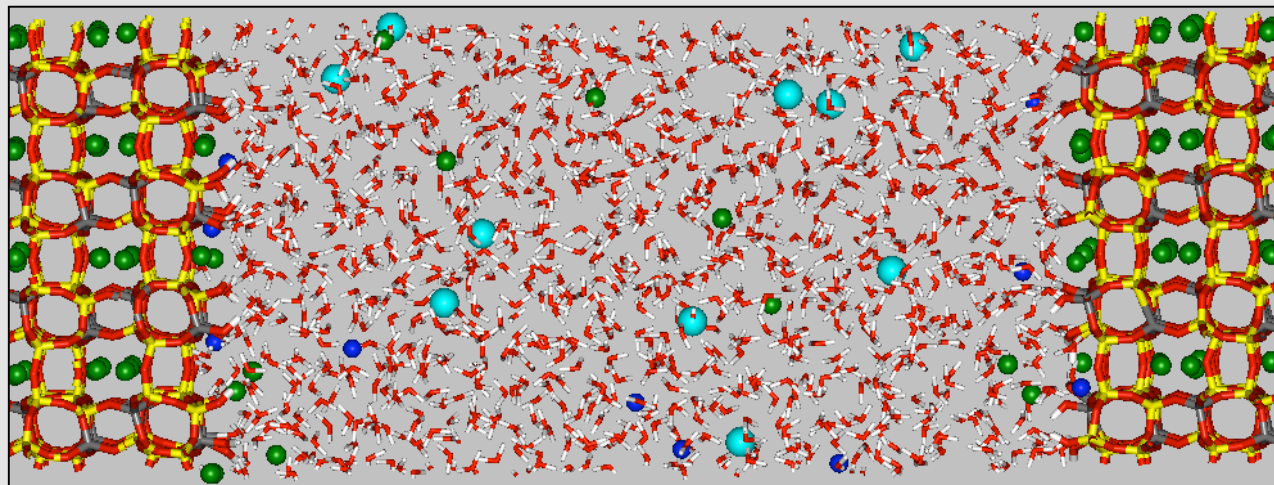
- **Two diffusion domains with distinct diffusion coefficients;**
- **Tortuosity factor ($\tau = D_p/D_{\text{H}_2\text{O}}$): 0.66 for fast domain
0.006 for slow domain;**

MD Simulation of Ion Diffusion

K-feldspar(001)

Fracture space

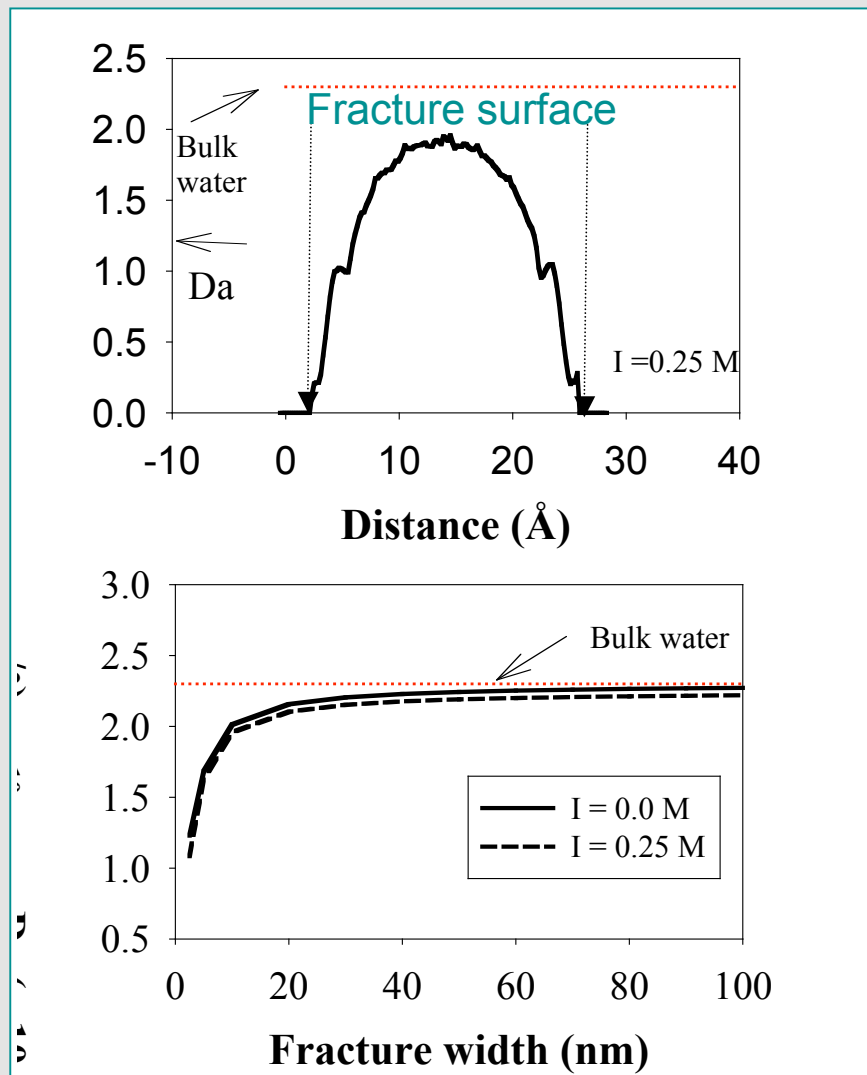
K-feldspar(001)



- Potassium
- Oxygen
- Hydrogen
- Silicon
- Aluminum
- Sodium
- Chlorine

$I = 0.5 \text{ M NaCl}$

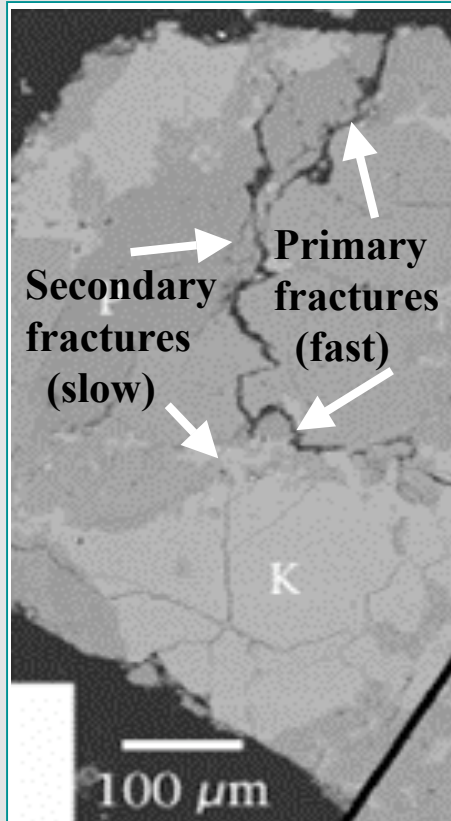
H₂O Diffusivity from MD Simulations



- Calculated diffusivity decreases toward fracture surface.
- Average diffusion coefficient within a fracture increases with increasing fracture width.
- The effect of fracture surfaces disappears when fracture width is over 100 nm.

Microscopic Mass Transfer Model

Working Model



Primary fractures: “fracture”
 Secondary fractures: “matrix”

Mathematical Equations

Reactive diffusion in matrix

$$\frac{\partial c_i^m}{\partial t} = \sum_{k=1}^N \frac{\partial}{\partial x} \left(D_{ik}^m \frac{\partial c_k^m}{\partial x} \right) + r_i^m \quad i = 1, 2, \dots, N$$

Reactive diffusion in fraction

$$\frac{\partial c_i^f}{\partial t} = \sum_{k=1}^N \frac{\partial}{\partial l} \left(D_{ik}^f \frac{\partial c_k^f}{\partial l} \right) + f_m \sum_{k=1}^N D_{ik}^m \frac{\partial c_k^m}{\partial x} \Big|_{x=0} + r_i^f$$

Scaling equations

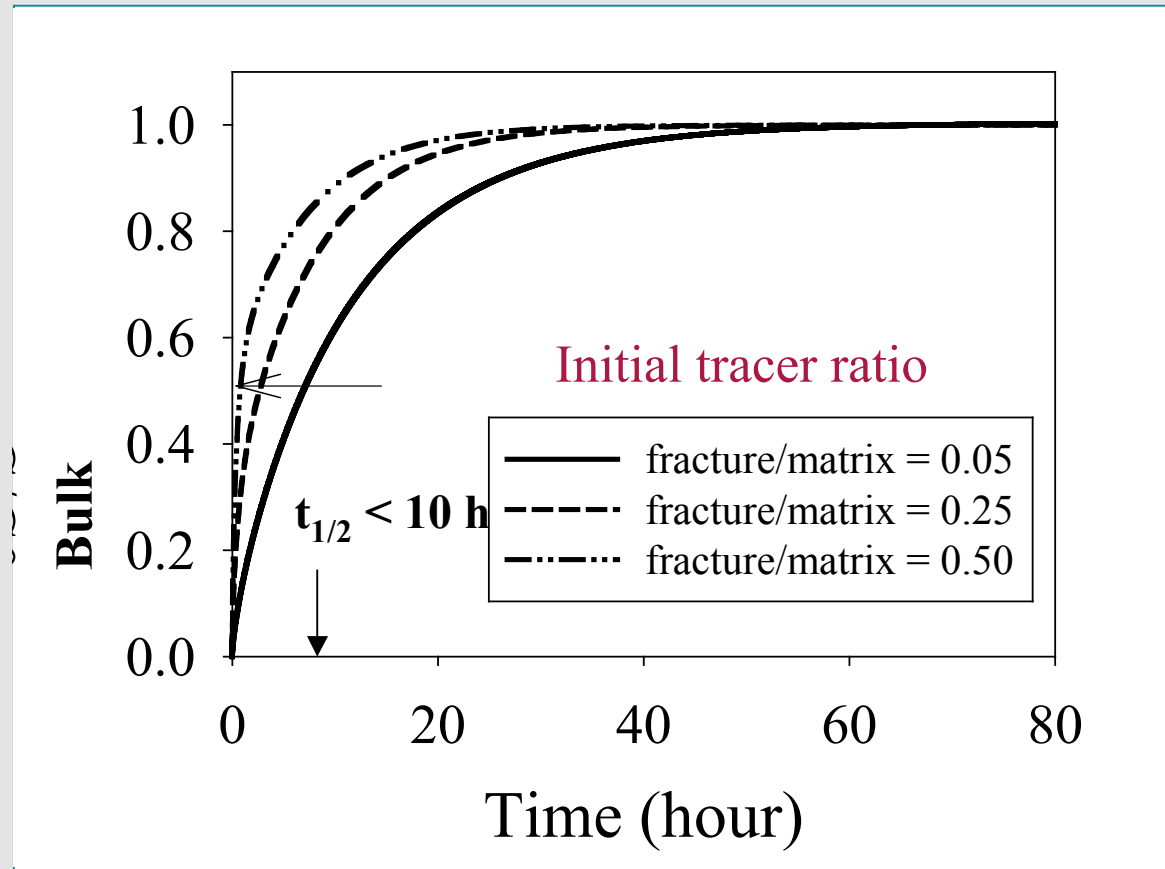
$$D_{ik} = \tau \left(D_i \delta_{ik} - \frac{Z_i Z_k D_i D_k c_i}{\sum_{k=1}^N Z_k^2 c_k D_k} \right)$$

D_i : molecular diffusion coefficient in water;
 τ : apparent tortuosity

$$\frac{\partial c_i^b}{\partial t} = AD + \frac{\theta_f}{\theta} \sum_{i=1}^N D_{ik}^f \frac{\partial c_k^f}{\partial l} \Big|_{l=0} + r_i^b$$

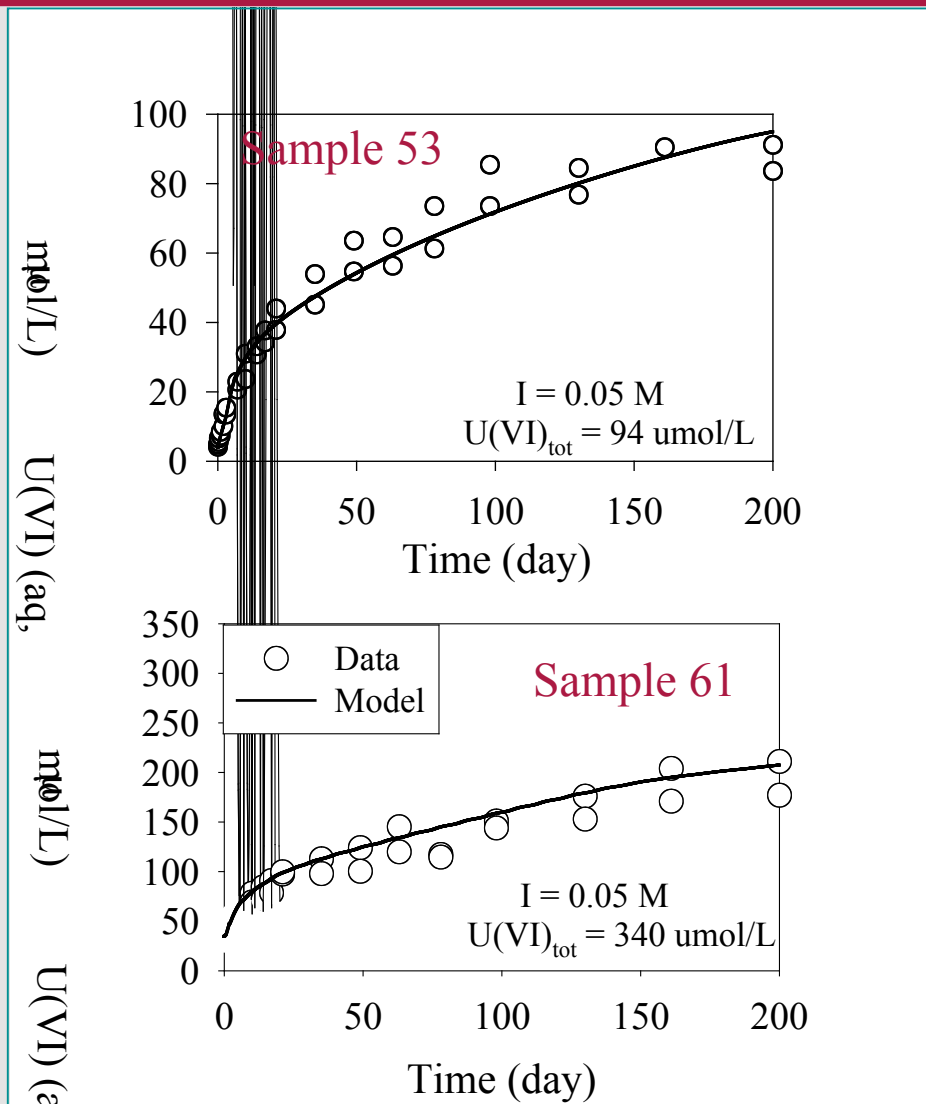
θ : mobile porosity;
 θ_f : fracture porosity.

Tracer Release from Sediment Fracture-Matrix



➤ Diffusion is NOT rate-limiting.

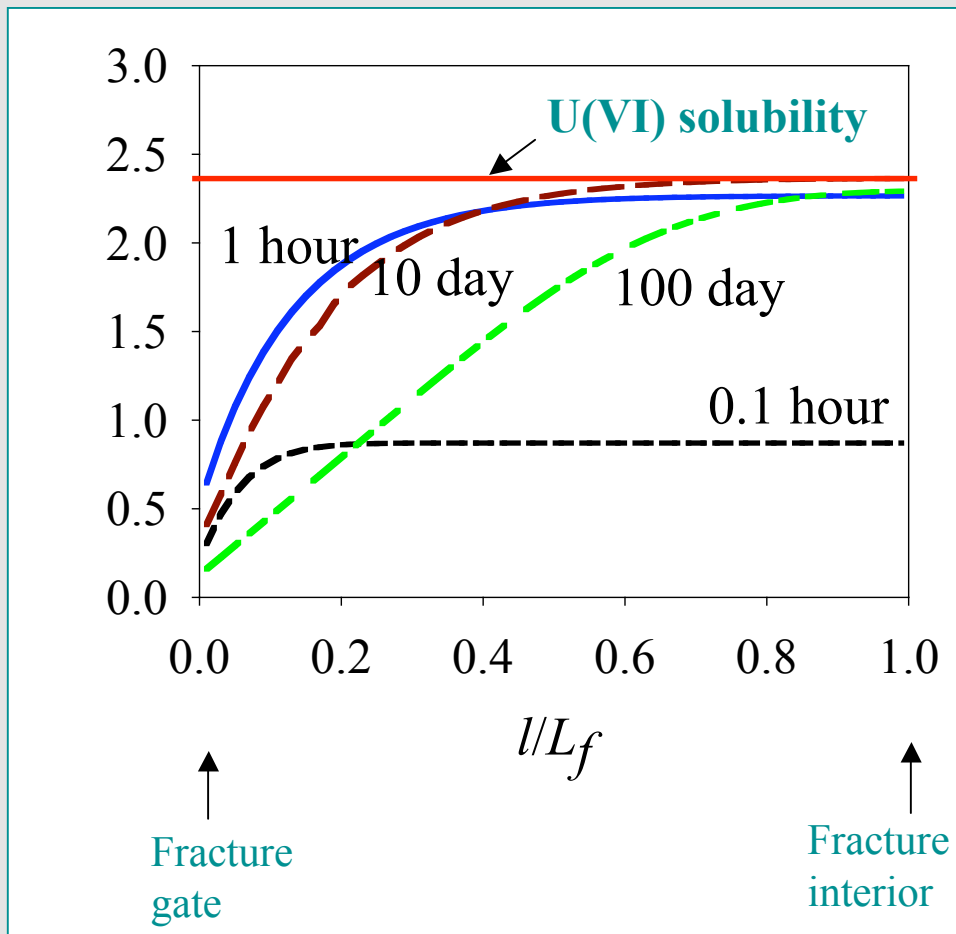
Coupled Diffusion and Dissolution



- Initial fracture/matrix $U(VI) = 0.25$ for sample 53; $= 0.08$ for sample 61
- The coupling of two relative fast processes: diffusion and dissolution, was able to describe a slower overall process: $U(VI)$ release from the sediments.
- Diffusion and dissolution mutually constrained.

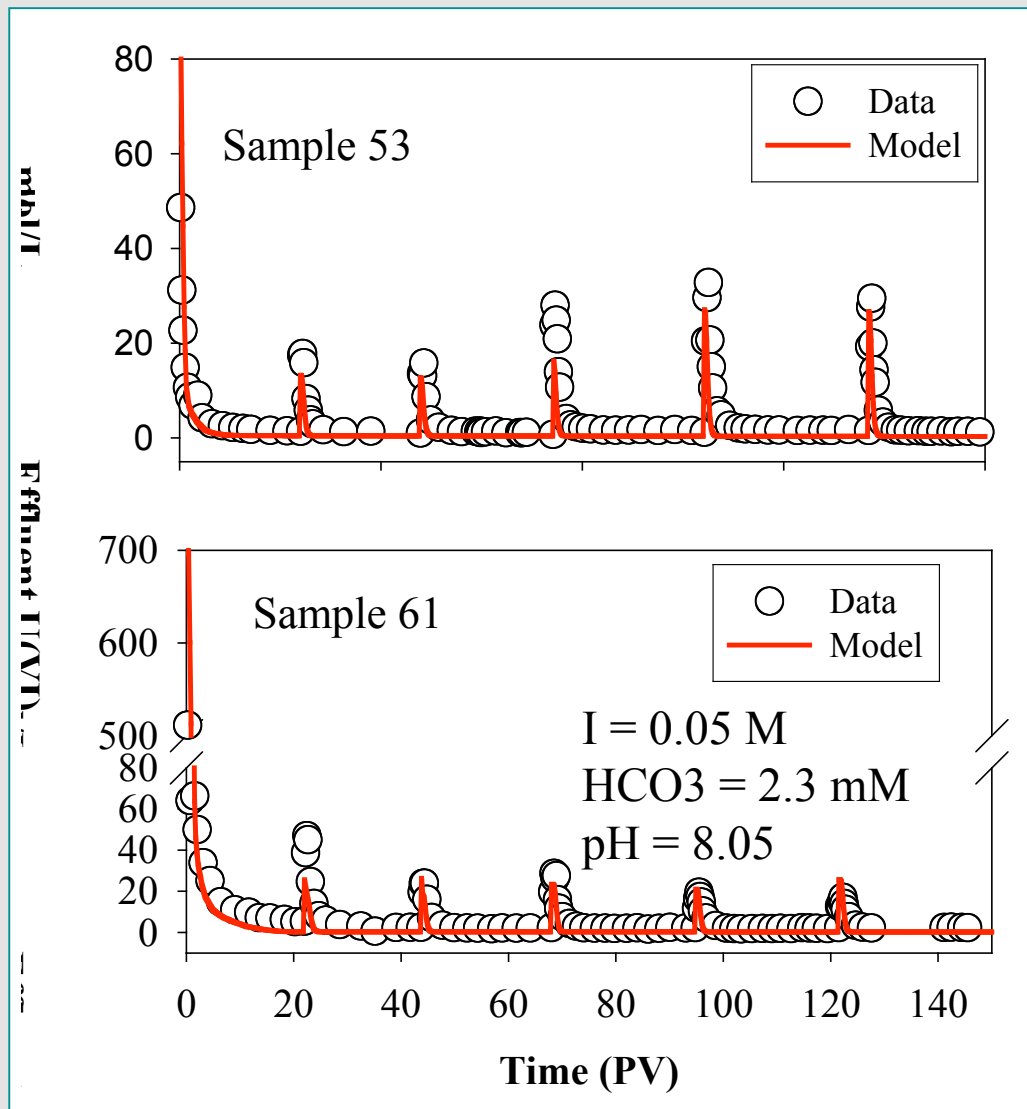
Coupled Diffusion and Dissolution

Aqueous U(VI) concentration in fracture



- Diffusion restricted the removal of local products of U(VI) dissolution, which decreased the rate of U(VI) dissolution because of the solubility limitation;
- Solubility restricted local U(VI) concentrations, which decreased diffusion gradients, and thus slowed the diffusion rates.

Advective Removal of U(VI) from Sediments



Conclusion and Implication

- ▶ **The rate of the coupled diffusion and dissolution reaction could be much slower than the individual processes, indicating the importance of process coupling. Implications: a) general dissolution reaction; b) sediment as a long-term U source.**
- ▶ **Multi-diffusion coefficients are apparently needed to describe intragrain diffusion, resulting from variable size and surface property of intragrain fractures. Implication: time-variable U(VI) release rates.**
- ▶ **Most of intragrain U(VI) in Hanford 200A sediments was associated with the slower diffusion region, indicating microscopic mass transfer will be an important process in controlling future U(VI) reactivity and stability.**

Acknowledgements: Funding support from US DOE ERSP. NMR measurements, MD simulation, and reactive diffusion modeling were performed at EMSL, a national scientific user facility sponsored by the DOE's Office of Biological and Environmental Research and located at the PNNL.

Thank You